Published OnlineFirst March 20, 2018; DOI: 10.1158/0008-5472.CAN-17-1900

Population and Prevention Science

Cancer Research

Germline Lysine-Specific Demethylase 1 (*LSD1/KDM1A*) Mutations Confer Susceptibility to Multiple Myeloma

Xiaomu Wei[1,2], M. Nieves Calvo-Vidal[1], Siwei Chen[2], Gang Wu[3], Maria V. Revuelta[1], Jian Sun[1], Jinghui Zhang[3], Michael F. Walsh[4], Kim E. Nichols[3], Vijai Joseph[4], Carrie Snyder[5], Celine M. Vachon[6], James D. McKay[7], Shu-Ping Wang[8], David S. Jayabalan[1], Lauren M. Jacobs[4], Dina Becirovic[5], Rosalie G. Waller[9], Mykyta Artomov[10], Agnes Viale[4], Jayeshkumar Patel[1], Jude Phillip[1], Selina Chen-Kiang[1], Karen Curtin[9], Mohamed Salama[9], Djordje Atanackovic[9], Ruben Niesvizky[1], Ola Landgren[4], Susan L. Slager[6], Lucy A. Godley[11], Jane Churpek[11], Judy E. Garber[12], Kenneth C. Anderson[12], Mark J. Daly[10], Robert G. Roeder[8], Charles Dumontet[7], Henry T. Lynch[5], Charles G. Mullighan[3], Nicola J. Camp[9], Kenneth Offit[4], Robert J. Klein[13], Haiyuan Yu[2], Leandro Cerchietti[1], and Steven M. Lipkin[1]

Abstract

Given the frequent and largely incurable occurrence of multiple myeloma, identification of germline genetic mutations that predispose cells to multiple myeloma may provide insight into disease etiology and the developmental mechanisms of its cell of origin, the plasma cell (PC). Here, we identified familial and early-onset multiple myeloma kindreds with truncating mutations in lysine-specific demethylase 1 (LSD1/KDM1A), an epigenetic transcriptional repressor that primarily demethylates histone H3 on lysine 4 and regulates hematopoietic stem cell self-renewal. In addition, we found higher rates of germline truncating and predicted deleterious missense KDM1A mutations in patients with multiple myeloma unselected for family history compared with controls. Both monoclonal gammopathy of undetermined significance (MGUS) and multiple myeloma cells have significantly lower KDM1A transcript levels compared with normal PCs. Transcriptome analysis of multiple myeloma cells from KDM1A mutation carriers shows enrichment of pathways and MYC target genes previously associated with myeloma pathogenesis. In mice, antigen challenge followed by pharmacologic inhibition of KDM1A promoted PC expansion, enhanced secondary immune response, elicited appearance of serum paraprotein, and mediated upregulation of MYC transcriptional targets. These changes are consistent with the development of MGUS. Collectively, our findings show that KDM1A is the first autosomal-dominant multiple myeloma germline predisposition gene providing new insights into its mechanistic roles as a tumor suppressor during post-germinal center B-cell differentiation.

Significance: KDM1A is the first germline autosomal dominant predisposition gene identified in multiple myeloma and provides new insights into multiple myeloma etiology and the mechanistic role of KDM1A as a tumor suppressor during post-germinal center B-cell differentiation. *Cancer Res; 78(10); 2747–59. ©2018 AACR.*

Introduction

In multiple myeloma, abnormal plasma cells (PC) derived from post-germinal center B cells abnormally proliferate and produce high amounts of immunoglobulin or paraprotein, which leads to lytic bone lesions, anemia, and renal failure (1). Multiple myeloma is preceded by a premalignant condition, monoclonal gammopathy of undetermined significance (MGUS). Consistent with genetic predisposition, having a first-degree relative with multiple myeloma elevates multiple myeloma risk 2- to 5.5-fold (2).

[1]Department of Medicine, Weill Cornell Medicine, New York, New York. [2]Department of Biological Statistics and Computational Biology, Weill Institute for Cell and Molecular Biology, Cornell University, Ithaca, New York. [3]St. Jude Children's Research Hospital, Memphis, Tennessee. [4]Memorial Sloan-Kettering Cancer Center, New York, New York. [5]Creighton University, Omaha, Nebraska. [6]Mayo Clinic, Rochester, Minnesota. [7]Cancer Research Center of Lyon, Lyon, France. [8]Rockefeller University, New York, New York. [9]University of Utah, Salt Lake City, Utah. [10]Analytic and Translational Genetics Unit, Massachusetts General Hospital, Boston, Massachusetts. [11]University of Chicago, Chicago, Illinois. [12]Dana-Farber Cancer Institute, Boston, Massachusetts. [13]Icahn School of Medicine, New York, New York.

Note: Supplementary data for this article are available at Cancer Research Online (http://cancerres.aacrjournals.org/).

X. Wei and M.N. Calvo-Vidal are co-first authors of this article.

Corresponding Authors: Steven M. Lipkin, Department of Medicine, Weill Cornell Medicine, 413 East 69th St., Belfer Rm 702, New York, NY 10021. Phone: 646-962-6303; Fax: 646-962-6302; E-mail: stl2012@med.cornell.edu; Nicola J. Camp, University of Utah School of Medicine, Salt Lake City, UT 84132. E-mail: Nicola.Camp@hci.utah.edu; Robert J. Klein, Icahn School of Medicine at Mount Sinai, New York, NY 10029. E-mail: robert.klein@mssm.edu; Haiyuan Yu, Cornell University, Ithaca, New York 14850. E-mail: haiyuan.yu@cornell.edu; and Leandro Cerchietti, Weill Cornell Medical College and New York Presbyterian Hospital, 525 East 68th Street, New York, NY 10065. E-mail: lec2010@med.cornell.edu

doi: 10.1158/0008-5472.CAN-17-1900

Published OnlineFirst March 20, 2018; DOI: 10.1158/0008-5472.CAN-17-1900

Identifying multiple myeloma predisposition genes can provide mechanistic insights into MGUS, myeloma pathogenesis, and PC differentiation. Genome-wide association studies have identified 16 common variants at loci significantly associated with multiple myeloma risk (3–8). However, the role of rare multiple myeloma high-penetrance predisposing genes is poorly understood. To identify multiple myeloma predisposition genes, we performed germline whole-exome sequencing (WES) for familial multiple myeloma probands and identified kindreds that carry germline truncating mutations in lysine (K)-specific demethylase 1 (*KDM1A*, also called LSD1; ref. 9). *KDM1A* is an epigenetic transcriptional repressor that primarily demethylates monomethylated and dimethylated histone H3 on lysine 4 (H3K4me1/me2) to repress target gene promoters and enhancers (10–12).

We used CRISPR to introduce a "second hit" mutation in lymphoblastoid B cells from a germline *KDM1A* mutation carrier, which increased H3K4me1 levels. MGUS and multiple myeloma cells have significantly lower *KDM1A* transcript levels compared with normal PCs, and may be particularly sensitive to *KDM1A* mutations causing loss of function or haploinsufficiency. We also performed mutation burden test analysis of patients with multiple myeloma unselected for family history and controls, which showed higher rates of germline *KDM1A* mutations in patients with multiple myeloma. Mice treated with a *KDM1A* small-molecule inhibitor, GSK-LSD1, have enhanced secondary immune response with expansion of PCs, increased immunoglobulin production, and appearance of serum paraprotein. RNA sequencing (RNA-seq) analysis of these abnormal mouse PCs shows enrichment of *MYC* oncogene transcriptional targets. Transcriptomic analysis of multiple myeloma cells from *KDM1A* mutation carriers shows upregulation of the MYC target oncogene *Cyclin D2* and enrichment of pathways associated with both intrinsic multiple myeloma pathogenesis and extrinsic multiple myeloma–bone marrow microenvironment interactions. Our findings show that *KDM1A* is a novel germline predisposition gene for multiple myeloma and provide new insights into its mechanistic roles as a tumor suppressor in B cells.

Materials and Methods

Patient inclusion criteria

All patient studies were conducted in accordance with the U.S. Common Rule, after approval by an Institutional Review Board (IRB) at the respective recruiting institution. Informed written consent was obtained from all subjects. Familial multiple myeloma probands ($n = 50$; Supplementary Table S1) analyzed by exome sequencing met inclusion criteria: (i) confirmed diagnosis meeting revised criteria of the International Myeloma Working Group, (ii) IgG heavy/light chain analyzed, and (iii) $\geq$1 first-degree or $\geq$2 second-degree relatives diagnosed with multiple myeloma. KDM1A-Sanger sequencing European ancestry (EA) validation cohort ($n = 400$) inclusion criteria were: (i–iii; $N = 200$) or (i), (ii), and (iv) multiple myeloma onset younger than 60 years ($n = 200$).

Whole-exome sequencing

Germline DNA extracted from peripheral blood was used for whole exome capture using Agilent SureSelect 38 Mb paired-end sequencing and ran on Illumina HiSeq 2000s/2500s. FASTQ files were aligned to human reference genome (GRCh37) to generate BAM files using BWA v0.7.12. Picard tools were used for quality metric calculation and marking duplicate reads. GATK version 3.5-0-g36282e4 was used for variant calling using the haplotype caller algorithm. Variant quality score recalibrated (VQSR) data were used for filtering variants. Variant-level and interval-level annotations used SNPEff, ANNOVAR, and CAVA programs. Downstream analysis consisted of filtering out low-quality variant calls and common variants. Average coverage depth was 80×–100×. Variants with read depth (DP) of 10 or greater and a genotype quality (GQ) score of 20 or greater were included in analyses. Variant-, exon-, and gene-level data were obtained using information from the 1000 Genomes Project, NHBLI GO Exome Sequencing Project Exome Variant Server (EVS), Exome Aggregation Consortium (ExAC), and the combined annotation dependent depletion (CADD) server (13). Deleterious variants were defined as loss-of-function (frameshift insertion or deletion, stop-gain, splice-site change) or missense variants with CADD score >15. We performed segregation analysis using either exomes from family members or targeted Sanger sequencing. Cosegregating qualifying variants in Family 1 (Fig. 1A) shared by exomes are listed in Supplementary Table S2. Exome sequencing data can be accessed at NCBI (NCBI SRR5641111).

Sanger sequencing

For the *KDM1A*-Sanger sequencing EA validation cohort, all coding regions of *KDM1A* (NM_015013) were amplified using primers available upon request. PCR amplicons were sequenced in the Applied Biosystems 3730 DNA (Applied Biosystems) Analyzer and analyzed using Mutation Surveyor (SoftGenetics). *KDM1A* mutations in probands and indicated family members (Fig. 1A) were verified by Sanger sequencing.

Cell culture

Cell culture methods used are described in Supplementary Data S1.

KDM1A knockout by CRISPR/Cas9

To generate biallelic *KDM1A* truncating mutations in lymphoblastoid (LCL) cells that carry the *KDM1A* c.805_806delAG (p.Arg269Aspfs*7) heterozygous mutation, CRISPR/Cas9 gene editing sgRNA sequences were designed to target genomic sites near *KDM1A* c.805_806delAG (p.Arg269Aspfs*7). pX458_sgRNA (5′-CACCGTCAACTTC-GGCATCTATAAG-3′, 5′- AAACCTTATAGAT-GCCGAAGTTGAC-3′) was transfected into LCLs (Amax Nucleofector II device). GFP-expressing clones were seeded as single-cell clones in 96-well plates using flow cytometry and screened for mutations by PCR amplification, target sequencing, and Western blot analysis.

Western blot analysis and antibodies

LCL cells were harvested in lysis buffer containing complete Protease inhibitors (Roche, 4693159001). Whole-cell extracts were subjected to SDS-PAGE. Antibodies used include anti-H3K4me1 (Abcam ab8895, 1:500 dilution), anti-H3K4me2 (Abcam ab32356, 1:500 dilution), anti-H3K9me1 (Abcam ab9045, 1:500 dilution), anti-H3K9me2 (Abcam ab1220, 1:500 dilution), anti-Histone H3 (Abcam ab1791, 1:1000 dilution), anti-γ-tubulin (Sigma T5192), and anti-KDM1A (Santa Cruz Biotechnology sc-398794, 1:200 dilution).

Digital droplet PCR

A Bio-Rad assay specific for detection of the *KDM1A* frameshift mutation was designed (forward primer: 5′ CGTCATGGTCT-TATCAACT3′; reverse primer: 5′ AGGAGG-TCCTTACTTGGT3′;

Published OnlineFirst March 20, 2018; DOI: 10.1158/0008-5472.CAN-17-1900

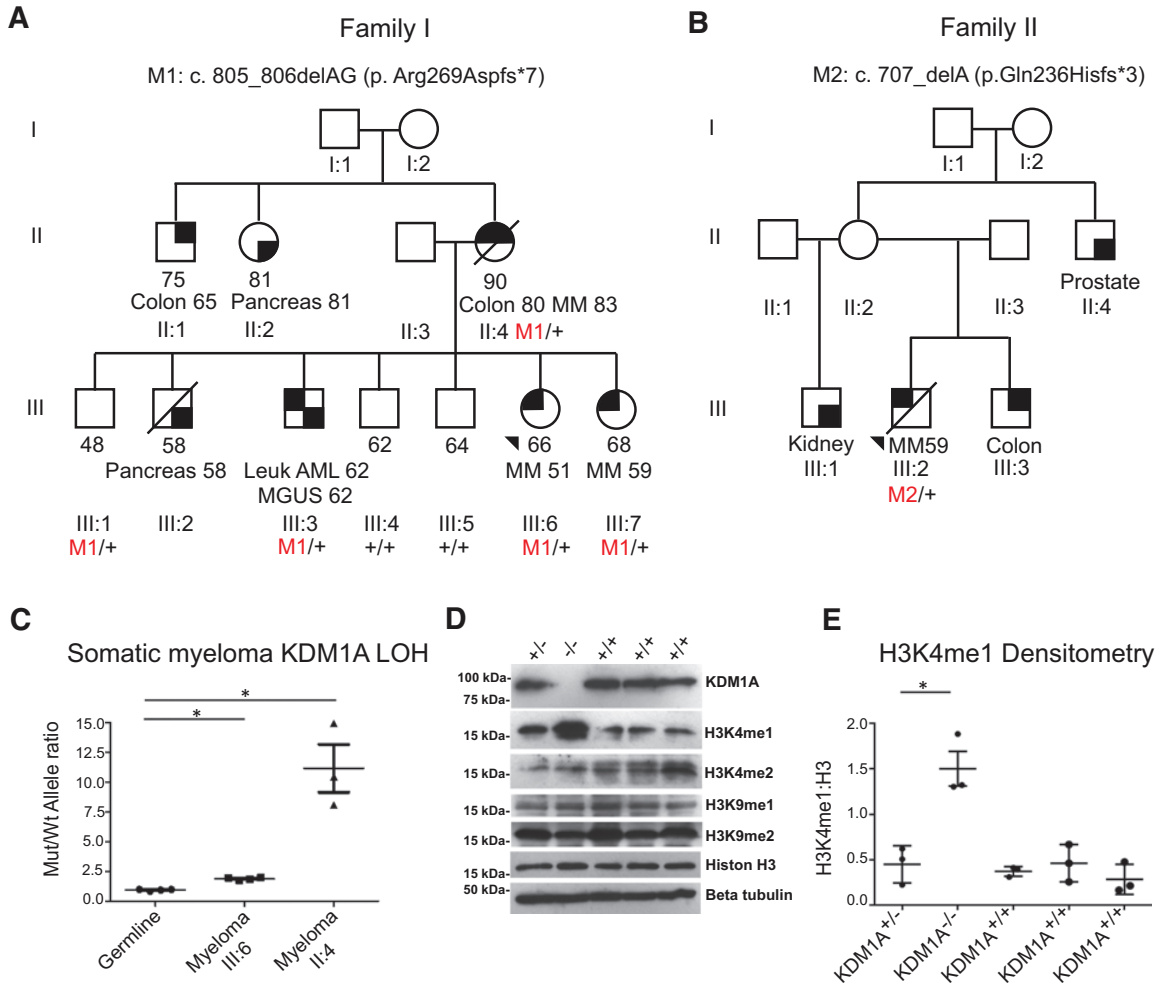

Figure 1.

Identification of germline *KDM1A* mutations in patients with familial and early-onset multiple myeloma. **A,** Pedigree of familial myeloma kindred carrying germline *KDM1A* c.805_806delAG (p.Arg269Aspfs*7) mutation. **B,** Pedigree of early-onset myeloma proband carrying *KDM1A* c.707delA (p.Gln236Hisfs*3) mutation. Last known ages, age of death if applicable, affected status with different malignancies, and ages at diagnosis are indicated. MM, multiple myeloma; AML, acute myeloid leukemia; Colon, colon cancer; Pancreas, pancreatic cancer; Prostate, prostate cancer; +, wild-type; M1 and M2, mutations. For kindred shown in **B**, only the proband had a biospecimen available for testing. For this kindred, ages of diagnosis for colon, kidney, and prostate cancers in family members could not be rigorously confirmed and so are not included. **C,** Somatic LOH in germline and myeloma cells from probands III:6 and II:4 in family carrying *KDM1A* c.805_806delAG (p. Arg269Aspfs*7) using digital droplet PCR. Ratio of *KDM1A* c.805_806delAG (p.Arg269Aspfs*7) mutant:wild-type allele for germline and myeloma cells is indicated with mean. *, $P < 0.01$ by Mann–Whitney test. $N = 3$ and 4, respectively. Mean and SEM are shown. **D** and **E,** Western blot and densitometry analysis showing *KDM1A* null (−/−) LCLs (generated from family member III:6 from the kindred shown in Fig. 1A) have undetectable KDM1A and increased H3K4 monomethylation (H3K4me1):H3 ratio. H3 dimethylated isoform (H3K4me2), H3, and tubulin are shown for comparison. Heterozygote and compound heterozygote LCLs were made from Family 1 III:6 (lanes 1 and 2) and wild-type LCLs were made from Family 1 II:3, III:4 and III:5 (lanes 3–5). Densitometry represents three independent measurements from each of the LCL cell lines. Mean and SEM are shown. *, $P = 0.015$ by two-tailed Student *t* test. LCL, B lymphoblastoid cell line.

Wt probe: 5′CGGCATCTATAagAGGATAAAACC3′-; mutation probe: 5′ CGGCATCTATAAGGATAAAACC3′. Cycling conditions were optimized for annealing/extension temperature and separation of positive from empty droplets on a QX200 ddPCR system (Bio-Rad). Technical duplicates were run. PCR reactions contain primers/probes, DNA, and digital PCR Supermix for probes (no dUTP). Reactions were partitioned into median approximately 16,000 droplets/well using QX200 droplet generator. Emulsified PCRs were run using cycling conditions (95°C 10 minutes; 40 cycles of 94°C 30 minutes 55°C 1′, 98°C 10 minutes, 4°C hold). Plates were read and analyzed with QuantaSoft software to assess the number of droplets positive for mutant DNA, wild-type (wt) DNA, both, or neither. Assay threshold sensitivity was set at 2 mutant droplets.

Mutation burden analysis

Exome data from 879 patients with sporadic multiple myeloma (dbGaP phs000748 and phs000348) and 2389 control

Published OnlineFirst March 20, 2018; DOI: 10.1158/0008-5472.CAN-17-1900

subjects (phs000179, phs000276, phs000403, phs000687, and phs000806) were simultaneously processed and variants jointly called. Exomes from cases/controls were required to have ≥75% of the 33.27 Mbps of CCDS with >10-fold coverage and ≤3% contamination using VerifyBamID (14). Exomes from cryptically related individuals were removed using KING algorithm (15). Principal component analysis (PCA) was performed using SMARTPCA (16) to identify EA. EA exomes meeting these quality control metrics were selected (733 patients with sporadic multiple myeloma and 1,480 controls). We compared the sum of (i) predicted deleterious mutation or (ii) neutral synonymous coding variant qualifying carriers for each gene in multiple myeloma cases and controls using Fisher exact test (statistical function scipy.stats.fisher_exact in SciPy v0.14.0.). Qualifying variant criteria include (i) a quality score (QUAL) ≥50, (ii) a genotype quality (GQ) score ≥20, (iii) a quality by depth (QD) score ≥2, (iv) a mapping quality (MQ) score ≥40, (v) a read position rank sum (RPRS) score ≥-3, (vi) mapping quality rank sum (MQRS) score ≥-10, and (vii) coding variants with mean allele frequency (MAF) ≤ 0.05% in all three databases of the 1000 Genomes Project, ESP, and ExAC. For rare synonymous variant burden testing, synonymous coding variants meeting criteria (i)–(vii) were used. For mutation burden testing, loss-of-function (frameshift insertion or deletion, stop-gain, splice-site change) and missense variants with Phred CADD score ≥15 meeting criteria (i)–(vii) were used. For association testing, common variants were required to meet criteria (i)–(vi), have MAF ≥5%, and be in Hardy–Weinberg equilibrium in cases, controls, and the combined group ($P > 0.001$ for each). PCA, rare synonymous, predicted mutation gene burden, and common variant association lambda statistics were used to confirm case–control matching and lack of notable population stratification (Fig. 2A–D; Supplementary Fig. S1).

Multiple myeloma organoids

Peg-Mal (polyethylene glycol-malate; AA peptides) hydrogels with REDV (AA peptides) peptidic ligands were impregnated with 30,000 U266 myeloma cells and 5,000 HS5 nonproliferating (mitomycin-treated) stromal cells, or 30,000 mononucleated cells from a primary bone marrow biopsy sample as previously described (17) with the addition of VLA-4/Integrin α4β1 ligand fibronectin (18). After gelation, hydrogel 3D organoids were rehydrated with media and cultured as described previously (17, 19). A detailed protocol for multiple myeloma organoid culture is available upon request. U266 organoids untreated or treated with 1 μmol/L LSD1 inhibitor (GSK-LSD1) were followed by microscopy. Cells were harvested and counted by measuring ATP content/well (CellTiter Glo, Promega) at days 0, 1, 3, 5, and 7. Three to five replications were used per organoid datapoint. For the primary bone marrow biopsy sample, after 6 days in culture, 2 organoids per experimental condition were mechanically digested and single cells assessed for PC markers CD138 and p63 using flow cytometry, and growth assessed at the same time point for 3 organoid datapoints per treatment condition using CellTiter Glo. To assess proliferation in a bone marrow sample of a patient with multiple myeloma in remission, mononuclear cells were preloaded with CellTrace Violet (Thermo Fisher Scientific).

RNA-seq analysis

For mouse PCs, polyadenylated single-read RNA-seq was performed using standard Illumina Truseq protocols and run at 3/lane on HiSeq 2500. Reads were trimmed of adapters with Flexbar then aligned to mm10 mouse genome (20). Uniquely mapped reads were used for read counts. Raw read counts were processed in R with DESeq2 (21) and accessed at NCBI (NCBI GEO GSE85596). Gene set enrichment analysis (GSEA) scores were calculated as the negative $\log_{10}$ of the false discovery rate (FDR) multiplied by the sign of the $\log_2$ fold change (log FC). Scores were run against preranked GSEA Hallmarks (weighted score type, 1,000 permutations; ref. 22) or Boylan multiple myeloma gene sets (23). Differentially expressed genes (DEG) were graphed as a volcano plot in R.

For analysis of MMRF CoMMpass RNA-seq multiple myeloma transcriptomes from *KDM1A* mutation carriers and patients with wt multiple myeloma, raw counts (19) were analyzed in R with DESeq2 (20). Multiple myeloma RNA-seq data were available from 4 *KDM1A* mutation carriers (MMRF_1201, 1730, 2293, and 2068). RNA-seq data from these 4 tumors were compared against 4 randomly picked multiple myeloma tumors from the 799 nonmutation carriers and run for 1,000 iterations. Significantly up- or downregulated genes ($P_{adj} < 0.05$) were compared against mouse GSK-LSD1–treated PCs. Outputs with >5% frequency were input for pathway enrichment in ClueGO (23), using GO Biological Process, Kyoto Encyclopedia of Genes and Genomes, REACTOME, and Wikipathways ontologies. Two-sided hypergeometric test was used to calculate *P* values, followed by Bonferroni correction. Pathways with $P_{adj} < 0.05$ were considered significant. The complete lists of genes and pathways are given in Supplementary Table S3.

For analysis of hypodiploid acute lymphoblastic leukemia (ALL) gene expression data (24), we compared samples with truncating *KDM1A* mutations (SJHYPO021 and SJHYPO032) to 50 *KDM1A* wt hypodiploid ALL tumors and used GSEA ($n = 1{,}000$ permutations) to test for enrichment of HoxA9 and LSK gene sets (25).

Mouse immunization and GSK-LSD1 treatment

C57BL/6 male mice aged 11 weeks ($n = 18$) were immunized intraperitoneally with 100 μg NP-CGG in alum on day 0 and day 21. On day 1, intraperitoneal treatment with either vehicle (PBS) or GSK-LSD1 (Cayman Chemical #16439; 0.5 mg/kg//day) started and continued until day 45. On days 10 and 35, mice were bled. On day 45, mice were sacrificed, and heart blood, femurs, and spleen were collected and analyzed.

Cell sorting and FACS

Mouse spleens were processed into single-cell suspensions, pooled in groups of 3–4, and washed before resuspending Ficoll-isolated mononuclear cells in PBS containing 0.5% BSA and antibodies B220-PECy7 (eBioscience, #25-0452-82) and CD138-APC (BD Pharmigen #558626). After one wash, 20 million cells/mL were resuspended and DAPI (1 μg/mL) added to exclude dead cells. Cells collected were $B220^+$ $CD138^-$ (B cells) and $CD138^+$ (PCs), and were >95% pure. Bone marrow samples extracted from mouse femurs and spleen mononuclear cells were also analyzed by FACS with B220, CD138, CD3, CD11b, and Gr1 antibodies.

NP-immunoglobulin ELISA and serum electrophoresis

Day 35 retro-orbital blood sera were serially diluted, incubated overnight in 96-well plates precoated with NP (4)-CGG or NP (27)-CGG (Biosearch, #N-5055A and N-5055C), and pre-blocked with PBS with 1% BSA. After three washes with 0.05% Tween-20 PBS, horseradish peroxidase–conjugated antibodies against IgG1, IgG2a, IgG2b, IgG3, IgM, or IgA (SouthernBiotech,

Published OnlineFirst March 20, 2018; DOI: 10.1158/0008-5472.CAN-17-1900

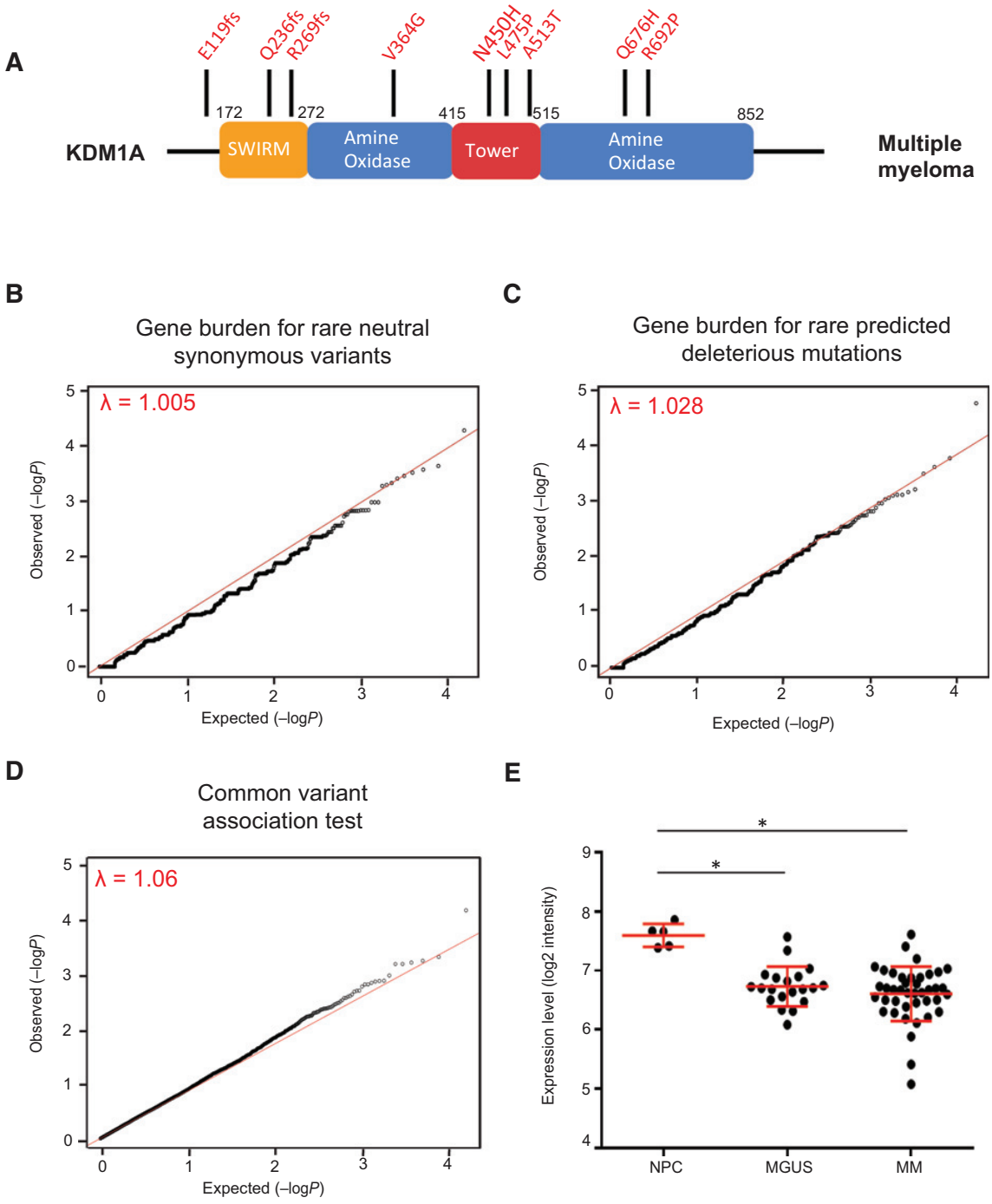

Figure 2.

KDM1A germline mutations in patients with multiple myeloma. **A,** Schematic of KDM1A protein. Germline mutations from patients with multiple myeloma are shown on top. **B** and **C,** Quantile–quantile plots of gene-based burden tests for rare neutral synonymous variants (**B**) and rare predicted deleterious mutations (**C**). **D,** Quantile–quantile plot of multiple myeloma case and control common variants. Lambda statistics are shown. **E,** *KDM1A* mRNA levels in normal plasma cells (NPC), MGUS, and multiple myeloma cells. *, $P = 7.45 \times 10^{-6}$ (NPC-MGUS) and 1.70×10^{-5} (NPC-MM), respectively, moderated *t* test. Mean and SEM bars are indicated.

Published OnlineFirst March 20, 2018; DOI: 10.1158/0008-5472.CAN-17-1900

#5300-05) were used to detect NP-specific antibodies. ABTS (SouthernBiotech, #0404-01) was used as peroxidase substrate and the reaction stopped with 1% SDS. Absorbance of the product was measured at 410 nm.

Serum electrophoresis (Helena Laboratories) in agarose was performed with day 45 heart blood sera. Densitometry-based quantification of serum protein bands was expressed as percentage of total protein in samples quantified in a Roche/Hitachi Modular P Chemistry Analyzer.

Study approval

Patients were consented under IRB-approved protocols in accord with CIOMS at Weill Cornell Medicine (New York, NY), Memorial Sloan-Kettering (New York, NY), Creighton University (Omaha, NE), University of Utah (Salt Lake City, UT), Mayo Clinic (Rochester, MN), Dana-Farber Cancer Institute (Boston, MA), and University of Lyon (Lyon, France). All mouse experiments were performed under Institutional Animal Care and Use Committee–approved protocols at Weill Cornell Medicine (New York, NY).

Statistical analysis

Statistical tests used are described in Supplementary Data S1.

Internet resources cited

Internet resources cited are listed in Supplementary Data S1.

Results

Germline truncating *KDM1A* mutations in familial multiple myeloma

Germline exome sequencing of 50 familial multiple myeloma kindreds (Supplementary Table S1) revealed EA family carrying a N-terminal truncating *KDM1A* mutation (c.805_806delAG [p.Arg269Aspfs*7]; Fig. 1A) absent in ClinVar or Exome Aggregation Consortium (ExAc) databases. This was the only kindred with a qualifying truncating mutation (Supplementary Table S2). Therefore, we focused follow-up on this family. Sanger sequencing identified five relatives carrying this *KDM1A* mutation. Three were multiple myeloma affected (II:4, III:6, and III:7), one (III:3) with both acute myelogenous leukemia (AML) and MGUS, and one unaffected at age 48 (III:1; Fig. 1A). Three additional family members were diagnosed with pancreatic (II:2, III:2) and colon cancers (II:1).

KDM1A is composed of three major domains: SWIRM and Tower, which mediate protein–protein interactions, and a C-terminal amine oxidase (AO) domain (26). The truncating *KDM1A* c.805_806delAG (p.Arg269Aspfs*7) mutation eliminates the AO and Tower domains. Western blot analysis of LCL derived from patient III:6 showed normal levels of full-length KDM1A and no truncated protein. RT-PCR and Sanger sequencing of cDNA revealed the absence of *KDM1A*-mutant transcripts.

Identification of germline truncating *KDM1A* mutations in early-onset multiple myeloma

We next sequenced *KDM1A* exons in 400 additional EA multiple myeloma early-onset (<age 60) or familial myeloma probands. This identified another EA patient with early-onset multiple myeloma (age 59) and a truncating *KDM1A* mutation (*KDM1A* c.707delA [p.Gln236Hisfs*3]) in the SWIRM domain (Fig. 1B). No other family members were diagnosed with multiple myeloma/MGUS. One sibling was affected with colorectal cancer, a half-sibling with renal cell cancer, and one uncle with prostate cancer.

CADD scoring is a widely used computational tool to predict whether germline variants are benign or deleterious (13). The higher a CADD score, the higher the likelihood that a genetic variant is deleterious. Using CADD $\geq$15 threshold we identified two predicted rare deleterious *KDM1A* missense mutations in the Tower and AO domains, (*KDM1A* c.1424T>C [p.Leu475Pro] and c.2003G>C [p.Arg692Pro]) in patients with multiple myeloma with the first-degree relatives also affected with multiple myeloma/MGUS. Collectively, these data confirm the presence of rare truncating and predicted deleterious missense *KDM1A* mutations in familial and patients with early-onset multiple myeloma.

To understand the prevalence of *KDM1A* truncating mutations in controls, we examined the ExAC database. Including all ethnicities only 9 predicted truncating and splice-site loss-of-function (LoF) variants were identified, carried by 10 individuals (10/60,694; LoF constraint metric pLI = 0.99). Seven of these are of EA. All *KDM1A* truncating mutations had mean allele frequencies $<1.6 \times 10^{-5}$ and no homozygotes were identified. Joint analysis of LoF mutations in familial and early-onset multiple myeloma cases (2/450) and ExAC EA participants as controls (7/36,664), showed enrichment of *KDM1A* LoF mutations among patients with familial and early-onset myeloma [$P = 0.005$, Fisher exact test; RR, 23.28; 95% confidence interval (CI), 4.85–111.75]. Overall, despite possible small mismatch in mean age and the precise definitions of our multiple myeloma probands and ExAC database assignments of EA, our data provide evidence of *KDM1A* LoF mutation enrichment in familial and early-onset multiple myeloma.

Digital droplet PCR analysis of germline *KDM1A*-mutant multiple myeloma cells

Myeloma cells from bone marrow biopsies were available for two members (II:4 and III:6) of the kindred carrying the *KDM1A* c.805_806delAG (p.Arg269Aspfs*7) mutation. Digital droplet PCR (ddPCR) was performed on DNA isolated from multiple myeloma cells and normal bone marrow. The *KDM1A* mutation was enriched in multiple myeloma cells from deletion of the wt allele compared with germline bone marrow cells carrying the heterozygous germline mutation in both family members tested [both $P < 0.01$, Mann–Whitney test (Fig. 1C)]. Next, we generated LCLs from members of this kindred carrying *KDM1A* heterozygous or wt genotypes. We used CRISPR/Cas9 gene editing technology to introduce a second hit on the wt allele and an LCL cell line was derived carrying biallelic *KDM1A* truncating mutations [(c.805_806delAG (p.Arg269Aspfs*7) and c.801_802insT (p.Lys268*)]. Western blot analysis of *KDM1A* biallelic (−/−), heterozygous (+/−), and wt (+/+) LCLs revealed that heterozygous and wt LCLs had similar *KDM1A* protein levels, but that biallelic mutant LCLs had no detectable KDM1A protein (Fig. 1D). Accordingly, $KDM1A^{-/-}$ LCLs have significantly higher overall cellular levels of H3K4me1, whereas total H3K4me2, H3K9me1, and H3K9me2 levels were not significantly changed (Fig. 1D and E).

Increased *KDM1A* mutations in sporadic patients with multiple myeloma

We performed gene burden tests using jointly called germline exomes from EA patients with multiple myeloma unselected for

Published OnlineFirst March 20, 2018; DOI: 10.1158/0008-5472.CAN-17-1900

family history and EA controls (Fig. 2A). Exomes were matched for quality metrics as before (27, 28), and KING algorithm used to exclude individuals with cryptic relatedness (15). PCA showed no apparent population stratification between EA multiple myeloma cases/controls (Supplementary Fig. S1). The distribution of neutral synonymous coding variants showed no significant difference in the number of genes carrying neutral synonymous coding variants in multiple myeloma cases ($N = 733$; yellow, average 17.55 ± 0.26/gene) and controls ($N = 1480$; blue, average 17.52 ± 0.18/gene; Mann–Whitney U test, $P = 0.91$; Supplementary Fig. S1). We used Fisher exact test (28, 29) to generate quantile–quantile plots for neutral synonymous coding variant and predicted deleterious coding mutation gene burden tests. We also used Fisher exact test to generate a quantile–quantile plot comparing multiple myeloma case and control common variants (MAF $\geq$ 5%). The genomic inflation factor (λ) statistic confirmed appropriate matching between multiple myeloma cases and controls ($\lambda = 1.005$, 1.028, and 1.06, respectively; Fig. 2B–D). This showed significant enrichment of *KDM1A* predicted deleterious missense and LoF/truncating mutations ($P = 1.27 \times 10^{-3}$) in patients with multiple myeloma compared with controls (Table 1).

Among patients with multiple myeloma, we detected another patient (56 years old) with early-onset multiple myeloma with an exon 2 splice-donor LoF/truncating mutation *KDM1A* c.517+1G>A, (p.Glu119Trpfs*15), but no LoF/truncating mutation in controls. The myeloma tumor from this patient carried a somatic deletion encompassing the entire *KDM1A* locus (chr1:830,800-120,666,600). In addition, screening for predicted deleterious *KDM1A* missense mutations with CADD scores $\geq$15 identified 8 patients with multiple myeloma with heterozygous-predicted deleterious missense mutations and 2 non-multiple myeloma control subjects (1.23% LoF/missense mutations in patients with multiple myeloma and 0.14% LoF/missense mutations in controls; RR, 9.08; 95% CI, 1.97–41.95; Table 1). The rate of predicted *KDM1A* LoF and missense mutations in EA controls is similar to the ExAc database (0.22%; 81/36,664). However, none of the 7 tumors from patients with multiple myeloma carrying *KDM1A* missense mutations whose tumor somatic mutation data were available demonstrated loss of heterozygosity (LOH; ref. 30).

We analyzed published transcriptome databases containing gene expression from normal PCs, MGUS, and multiple myeloma cells, and found that *KDM1A* mRNA levels are significantly lower in MGUS or multiple myeloma cells versus PC (7.45×10^{-6} and 1.7×10^{-05}, respectively, moderated t test; Fig. 2E; ref. 31). Overall, these data support a broader role for *KDM1A* inactivation in sporadic MGUS and multiple myeloma, in addition to its role in familial and early-onset multiple myeloma. Because they have significantly lower *KDM1A* levels compared with normal PCs, MGUS and multiple myeloma cells may be particularly vulnerable to epigenetic dysregulation from *KDM1A* haploinsufficiency or loss-of-function mutations.

KDM1A pharmacologic inhibition promotes expansion of multiple myeloma and PCs

To test a role of *KDM1A* in post-germinal center B-cell differentiation, we conducted antigen-driven B-cell differentiation *in vivo* experiments. To induce differentiation of B cells into PCs, we challenged immunologically mature C57BL/6 mice with T-cell–dependent antigens on day 1 and boosted at day 21. In one group of mice, we used sheep red blood cells (SRBC) as antigen and in another group NP-chicken gamma globulin (NP-CGG), which allows quantification of total and high-affinity immunoglobulins. KDM1A was inhibited with GSK-LSD1, an irreversible KDM1A inhibitor (Fig. 3A) with IC_{50} of 16 nmol/L that shows >1,000× selectivity for KDM1A over closely related FAD utilizing enzymes including LSD2, MAOA, and B. Mice were randomized to receive vehicle (PBS) or GSK-LSD1 0.5 mg/kg daily by intraperitoneal injection (Fig. 3B). Mice were monitored for primary (day 10) and secondary (day 35) antibody immune responses, and sacrificed (day 45).

Phenocopying the *Kdm1a* knockout mouse models (25, 32), GSK-LSD1 significantly decreased neutrophils and increased monocytes in bone marrow (Fig. 3C). Antigen-challenged mice treated with GSK-LSD1 showed increased splenic PCs (Fig. 3C). Analysis of serum total and high-affinity anti-NP antibody production revealed that KDM1A inhibition promoted secondary immune response to the T-cell–dependent antigen NP-CGG (Fig. 3D). KDM1A inhibition also promoted IgM to IgG2b isotype class-switching, a process where B cells activated upon antigen encounter are costimulated by Th cells (Fig. 3D). The increase in immunoglobulin production could be detected by serum electrophoresis as an increased gamma globulin fraction (Fig. 3E). These findings are consonant with a model whereby KDM1A activity is required to control abnormal generation and/or expansion of PC.

KDM1A inhibition promotes *in vivo* PC upregulation of *MYC* transcriptional targets

To characterize the transcriptional consequences of *KDM1A* inhibition in PCs, we performed RNA-sequencing of DEG in sorted PC ($CD138^+$) from GSK-LSD1 treated and control mice. To functionally categorize these genes, we conducted pathway analysis using GSEA (33) and identified "MYC targets (v1)" as a significant pathway associated with upregulated genes (Fig. 4A, $P = 0.0$, FDR = 0.0).

To evaluate mouse genes dysregulated by *Kdm1a* inhibition in PCs with development of multiple myeloma, we compared DEG in PCs from GSK-LSD1 treated versus control mice with Bcl-xL/Myc transgenic mouse multiple myeloma cells (23). GSEA showed enrichment of genes upregulated in Bcl-xL/Myc transgenic mouse multiple myeloma cells in GSK-LSD1–treated PC DEG (normalized enrichment score 1.64, $P = 0.0$, FDR 0.008; Fig. 4A), including Myc-driven multiple myeloma oncogenes *Ccnd1* and *Ccnd2* (Supplementary Table S3; refs. 34–36). Thus, Kdm1a pharmacologic inhibition enriched for upregulated MYC transcriptional targets including *Ccnd1* and *Ccnd2* as potential drivers of PC proliferation.

Table 1. Predicted deleterious KMD1A mutation frequencies in multiple myeloma probands and control subjects

Probands	Deleterious	Benign	Total	Mutation burden test (Fisher exact test)
Multiple myeloma	9 (1.23%)	724 (98.77%)	733	$P = 1.27 \times 10^{-3}$
Control subjects	2 (0.14%)	1,478 (99.86%)	1,480	
Total	11	2,202	2,213	

Published OnlineFirst March 20, 2018; DOI: 10.1158/0008-5472.CAN-17-1900

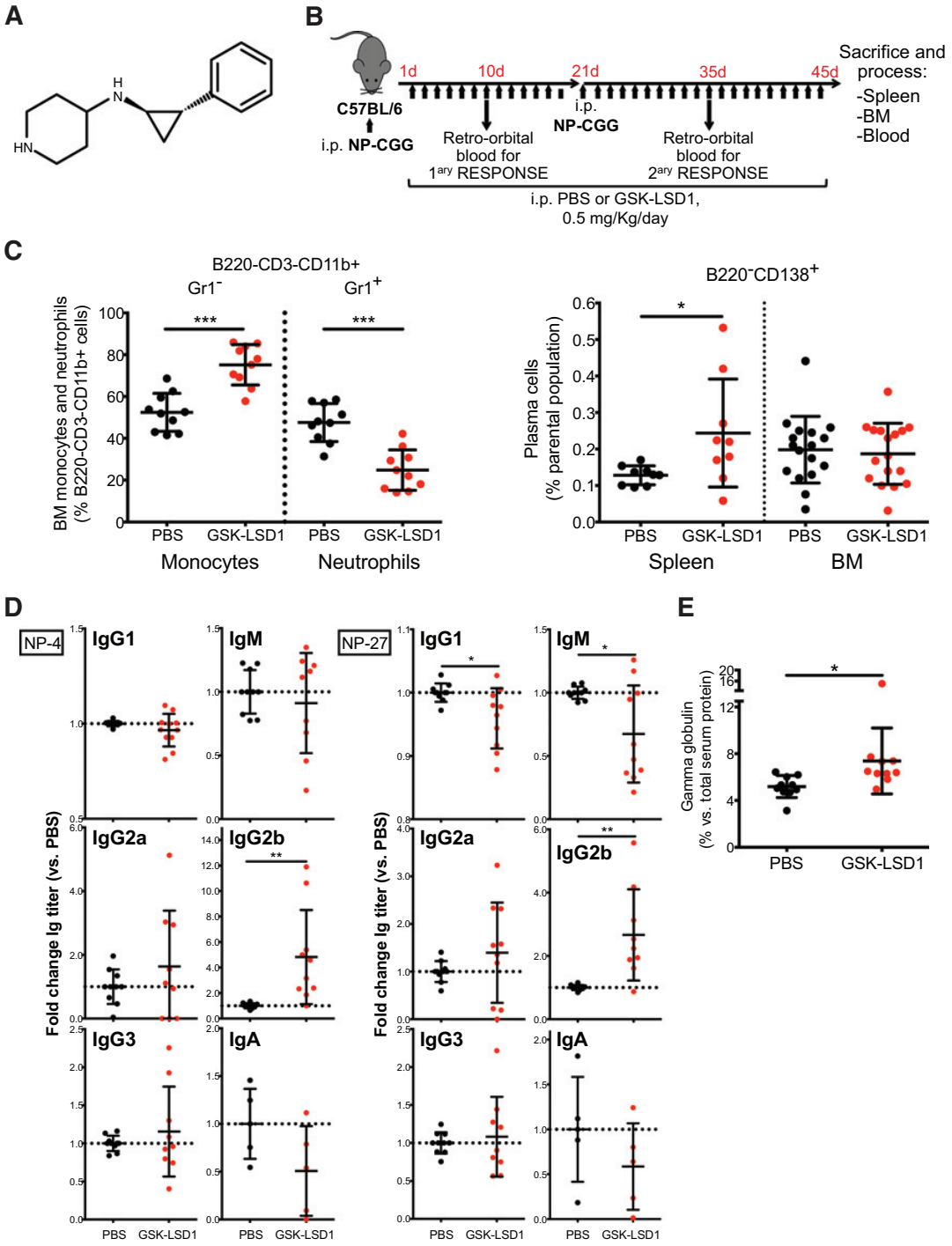

Figure 3.

KDM1A pharmacologic inhibition in mice promotes secondary immune response, immunoglobulin class switching, and serum paraprotein. **A,** Chemical structure of *KDM1A* inhibitor GSK-LSD1. **B,** Schedule of administration to mice and immune response elicited by antigen NP-CGG. **C,** Kdm1a inhibition recapitulates *Kdm1a*$^{-/-}$ mouse phenotype, with increased monocytes and reduced neutrophils in bone marrow (BM; left), and causes increased splenic PCs in the secondary immune response (right). At least $n = 9$ per condition. *, $P < 0.05$; ***, $P < 0.001$, Mann–Whitney test. Mean and SEM are shown. **D,** Kdm1a inhibition promotes NP-specific IgG2b antibodies production (high-affinity antibodies that detect the less haptenated antigen NP-4 and total antibodies that detect the highly haptenated antigen NP-27). At least $n = 5$ per condition. *, $P < 0.05$; **, $P < 0.01$, Mann–Whitney test. Mean and SEM are shown. **E,** Gamma globulin fraction in serum electrophoresis of same mice at day 45. $n = 10$ per condition. *, $P < 0.05$, Mann–Whitney test. Mean and SEM are shown.

Published OnlineFirst March 20, 2018; DOI: 10.1158/0008-5472.CAN-17-1900

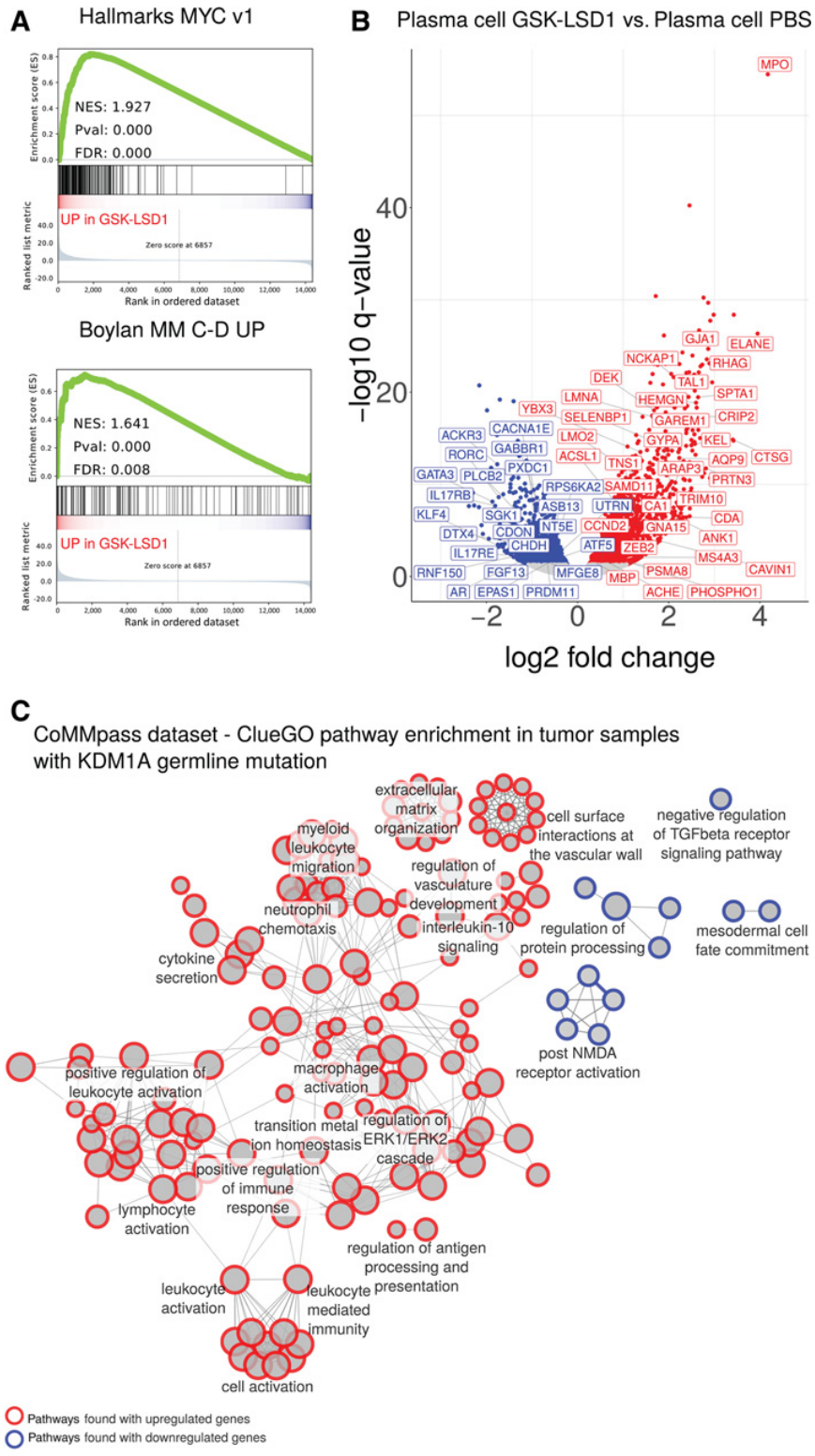

Figure 4.

KDM1A inhibition in mouse plasma cells and germline KDM1A mutations in patients with multiple myeloma alters gene expression. **A,** GSEA of differentially expressed genes in plasma cells from mice treated with GSK-LSD1 in MYC v1 MSigDB Hallmark (top) and Bcl-xL/Myc transgenic mouse multiple myeloma (bottom) gene sets. NES, normalized enrichment score. **B,** Volcano plot of differentially expressed genes in sorted plasma cells from mice treated with GSK-LSD1. Labels (human nomenclature) indicate genes differentially regulated in common for both GSK-LSD1–treated mouse PCs and multiple myeloma tumors from KDM1A germline predicted mutation carriers. **C,** ClueGO analysis pathways enriched in DEGs comparing multiple myeloma tumors from KDM1A germline mutation carriers to those from wild-type patients. Pathways with adjusted $P_{adj} < 0.05$ are shown. Circles, pathways. Size represents the percentage of genes shared with a pathway. Red, upregulated gene pathways; blue, downregulated gene pathways. Edges (lines) indicate shared genes between pathways.

Published OnlineFirst March 20, 2018; DOI: 10.1158/0008-5472.CAN-17-1900

Increased *CCND2* and alterations in other pathways in multiple myeloma cells from *KDM1A* mutation carriers

To determine the impact of germline *KDM1A* mutations on patient multiple myeloma tumors, we compared multiple myeloma tumor transcriptomes from patients with *KDM1A*-predicted deleterious mutations to those from *KDM1A* wt patients. First, we evaluated shared DEG common to both (i) GSK-LSD1–treated PCs and (ii) multiple myeloma cells from *KDM1A* mutation carriers versus wt patients. Upregulated shared DEG included *CCND2* (Fig. 4B). Among downregulated shared DEG were the transcription factor *KLF4* that has tumor suppressor functions in multiple myeloma (37) and *PRDM11*, a tumor suppressor in MYC-driven B lymphomagenesis (Fig. 4B; ref. 38). Thus, *CCND2*, *KLF4*, and *PRDM11* are potential transcriptional targets downstream of *KDM1A* whose dysregulation promotes MGUS and multiple myeloma in patients.

We then analyzed DEG in multiple myeloma tumors from *KDM1A* mutation carriers compared with wt patients by ClueGO pathway analysis (Fig. 4C; ref. 39). Pathways related to myelomagenesis enriched in upregulated genes include Immunoglobulin Production, Antigen Processing, and Presentation (40), IL10 signaling (41), ERK Signaling Cascade (42), Vasculature

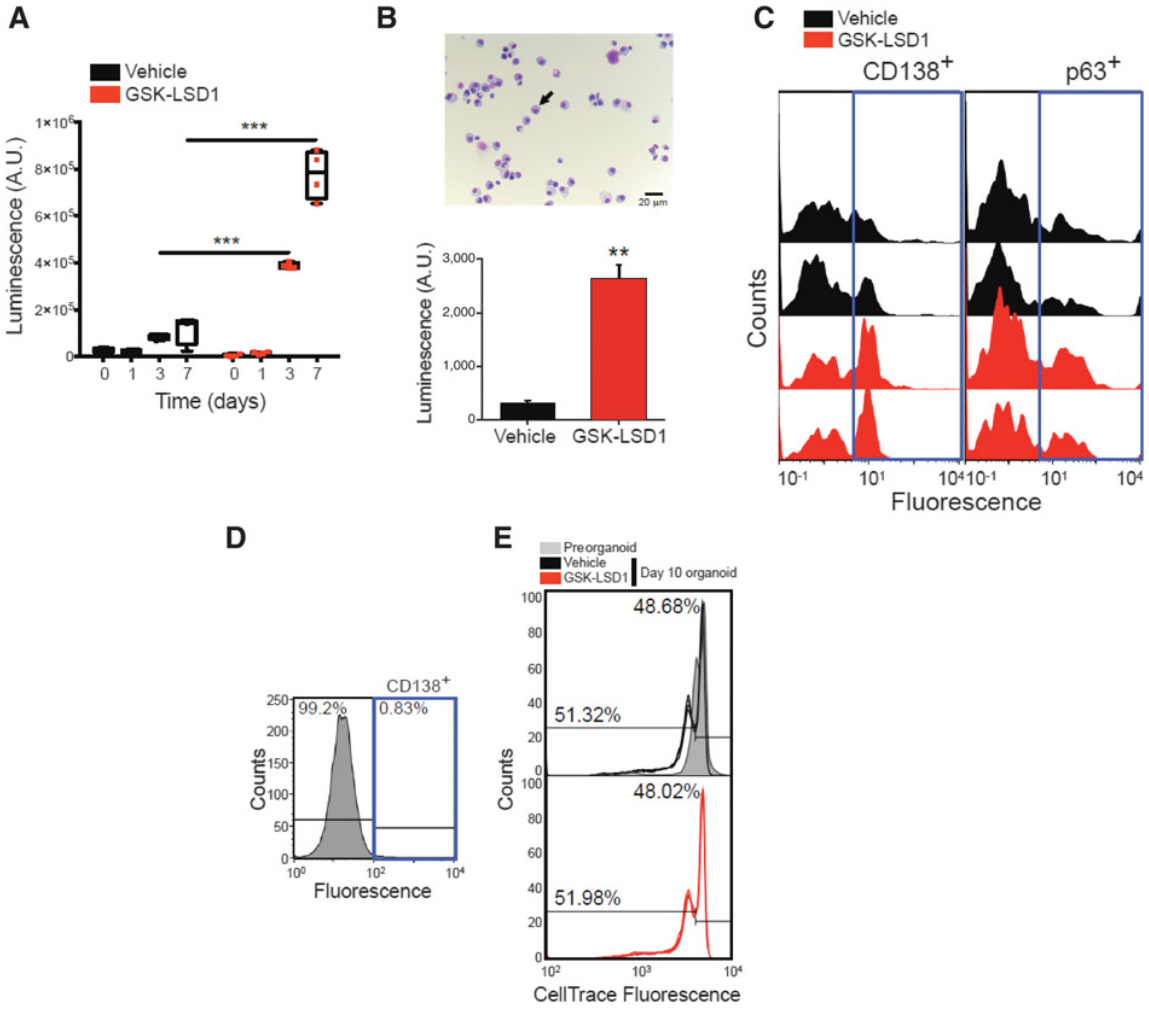

Figure 5.

KDM1A inhibition increases multiple myeloma cell line and primary patient culture cell proliferation in 3D cultures. **A,** 3D organoids containing an inert matrix presenting ligands for integrin α4β1 and U266 multiple myeloma cells were treated with vehicle or 1 µmol/L GSK-LSD1 for the indicated time points. Cell number was determined by contrast microscopy (not shown) and ATP content (CellTiter Glo). Experiment was performed with 3–5 replicates. ***, $P < 0.01$ Mann–Whitney test. **B,** Bone marrow aspirate from an untreated patient with multiple myeloma presented 90% plasma cells (black arrow) after 3 days of culture in flask (top). 3D organoids containing an inert matrix presenting ligands for integrin α4β1 and the 3-day cultured bone marrow aspirate were treated with vehicle or GSK-LSD1 1 µmol/L once at day 1. After 6 days of culture, total cell number was measured by ATP content (bottom). **, $P < 0.05$ Mann–Whitney test. **C,** Myeloma cell count from the same organoids in **B** as measured by FACS analysis of $CD138^+$ and $p63^+$ cells with FITC-conjugated antibodies. Left part of histograms corresponds to matrix debris and other non-PCs. **D,** Bone marrow aspirate from a patient with multiple myeloma in remission after 3 days of culture in flask. **E,** Bone marrow sample from **D** was loaded with the proliferation dye CellTrace Violet and cultured in 3D organoids for 10 days. Proliferation was assessed as a function of fluorescence decrease when compared with pre-organoid fluorescence.

Published OnlineFirst March 20, 2018; DOI: 10.1158/0008-5472.CAN-17-1900

Development (43), and Extracellular Matrix Organization (44), while in downregulated genes, the TGFβ signaling pathway was enriched (Fig. 4C). This included SMAD1, which suppresses MYC-dependent transcription in multiple myeloma cells (45). Altogether, these data reveal enrichment in pathways associated with both intrinsic multiple myeloma pathogenesis and multiple myeloma–bone marrow microenvironment interactions in *KDM1A* mutation carriers.

To directly test whether KDM1A affects myeloma cell proliferation, we treated human myeloma cells with GSK-LSD1 in 3D organoids with extracellular matrix–like biophysical properties that resemble the microenvironment of lymphoid tissues (17, 19). When U266 multiple myeloma cell line (Fig. 5A) or primary sporadic multiple myeloma patient cell (Fig. 5B and C) organoids were treated with GSK-LSD1, KDM1A inhibition significantly stimulated multiple myeloma cell number ($P < 0.001$ and <0.01, t test). In contrast, GSK-LSD1 treatment did not affect proliferation of nonmultiple myeloma $CD138^-$ bone marrow cells as controls (Fig. 5D and E). These data support roles for KDM1A regulating PC differentiation to prevent MGUS and multiple myeloma development, and also to promote multiple myeloma proliferation.

Discussion

MGUS and multiple myeloma risk is increased in relatives of affected individuals (2). We used whole-exome sequencing of familial myeloma kindreds, mutation cosegregation in family members, somatic tumor studies, CRISPR-induced somatic second hit mutations, targeted sequencing of additional patients with familial and early-onset multiple myeloma, mutation burden analysis in patients with multiple myeloma unselected for family history, multiple myeloma tumor transcriptome studies and functional studies of a KDM1A inhibitor on human multiple myeloma cells and mouse PC that promoted PC expansion, and increased immunoglobulin production and multiple myeloma cell proliferation to nominate *KDM1A* as the first autosomal-dominant multiple myeloma predisposition gene. Our data are consistent with germline *KDM1A* mutations predisposing to familial multiple myeloma, having a prevalence of approximately 1.23% in patients with multiple myeloma unselected for family history and conferring approximately 9-fold increased risk of developing multiple myeloma.

Whole body knockout or shRNA knockdown of mouse *Kdm1a* is embryonic lethal (25, 32). In hematopoietic cells, *Kdm1a* knockout/knockdown causes immature HSPC blasts, LSK progenitors, and monocytes to proliferate while LT-HSC, granulocytes, megakaryocytes, and erythrocytes are reduced (25, 32). The early lethality of *Kdm1a*-mutant mouse models has limited studies of B lymphocytes, which continue to be produced despite absent *Kdm1a* (25, 32). Therefore, the roles of *KDM1A* in B lymphocytes are poorly understood.

Previously, chronic exposure to lysolipid and dioxin antigens was proposed to drive the transition from PC to MGUS (46, 47). In mice, Kdm1A pharmacologic inhibition upregulates PC *MYC* proto-oncogene targets including *Ccnd1* and *Ccnd2*, increases PC numbers, high-affinity secondary immune response to T-cell–dependent antigens, immunoglobulin production and causes the appearance of serum paraprotein (Fig. 3C). On the basis of similarities between these PC and Bcl-xL/Myc–driven mouse multiple myeloma cells, this transcriptional dysregulation likely predisposes to additional myelomagenesis-driving events. Furthermore, analysis of tumor transcriptomes from *KDM1A*-mutant patients is consonant with selected alterations persisting in multiple myeloma cells, such as increased *CCND2* and reduced *KLF4* and *PRDM11* (37, 38). In line with multiple myeloma organoid findings, tumor transcriptomes from *KDM1A*-mutant patients are enriched in pathways associated with both intrinsic multiple myeloma pathogenesis and extrinsic multiple myeloma–bone marrow microenvironment interactions. These data are consistent with KDM1A inhibition/mutation acting at distinct steps to promote both PC immune response and multiple myeloma proliferation by dysregulating both cell-intrinsic (including MYC driven) and -extrinsic microenvironment signaling pathways.

We identified both *KDM1A* germline truncating and missense mutation carriers (Fig. 2). Somatic multiple myeloma tumor analyses performed with two members of our index family carrying a *KDM1A* truncating mutation (Fig. 1) showed evidence of possible LOH. However, this finding may be by chance, as chromosome 1p deletion is frequent in myeloma (1, 42). Of seven additional *KDM1A* predicted germline mutation carriers with somatic multiple myeloma mutation data, only one patient with multiple myeloma tumor showed somatic LOH. The other 6 patients with multiple myeloma without tumor LOH carried germline missense mutations. KDM1A is a component of the NuRD and CoRest chromatin remodeling complexes, and participates in multiple protein–protein interactions with distinct histone demethylase activities (10–12). It is possible that KDM1A missense mutations act through a dominant negative mechanism in PC NuRD or CoRest complexes to promote MGUS/multiple myeloma predisposition. Alternatively, because MGUS and multiple myeloma cells both have significantly lower KDM1A levels compared with normal PCs (Fig. 2E), they may be particularly vulnerable to epigenetic dysregulation from *KDM1A* hypomorphic missense mutations and haploinsufficiency.

Scales and colleagues recently reported a multiple myeloma exome mutation burden test study in 513 United Kingdom northern EA multiple myeloma cases from two clinical trials (48). While no individual gene reached genome-wide significance in this study, the authors nominated KIF18A as a promising multiple myeloma predisposition candidate. However, in our EA multiple myeloma mutation burden study, we did not see an association between KIF18A and multiple myeloma (Fisher exact test, $P = 0.787$). Furthermore, the study of Scales and colleagues did not nominate KDM1A as multiple myeloma predisposition gene. A likely reason for these different findings is that Scales and colleagues used variant MAF filter <1% while our study used MAF $\leq$0.05% to define rare candidate mutations. Thus, each study used different inputs for mutation burden testing. Additional potential reasons include methodologic differences in variant annotation and mutation burden testing pipelines, possible differences in EA population substructure (American vs. UK patients with multiple myeloma), and different rates of clinical covariates for patients with multiple myeloma and their tumor molecular subtypes.

Bolli and colleagues performed exome sequencing of a large, multiplex MM/MGUS kindred (49). The authors nominated EP300 and PDPK1, but not KDM1A, as candidate MGUS/multiple myeloma predisposition genes. However, in contrast to the KDM1A mutation carrying kindreds we identified (Fig. 1A and B), this family did not have non-multiple myeloma/MGUS cancers. Thus, additional MGUS/multiple myeloma specific high-risk predisposition genes may exist.

Published OnlineFirst March 20, 2018; DOI: 10.1158/0008-5472.CAN-17-1900

Recently, recurrent somatic KDM1A mutations were identified in chronic myeloid leukemia (50). We also identified one patient with a germline truncating *KDM1A* mutation diagnosed with MGUS and AML (Fig. 1A). In mice, *Kdm1a* knockout causes monocytosis (25, 32). However, *KDM1A* inhibition was found to induce terminal differentiation of AML cell lines and several primary AML cultures (51). On the basis of this, *KDM1A* small-molecule inhibitors are used in clinical trials for AML and other conditions. Our study of germline *KDM1A* mutations supports individuals being treated with KDM1A inhibitors being monitored for MGUS/multiple myeloma.

We also surveyed germline data from patients with pediatric hypodiploid ALL (24). This revealed a germline *KDM1A* truncating mutation c.1368_1371delAGAA (p.Lys456Asnfs*12) in a patient with near-haploid hypodiploid ALL whose tumor demonstrated LOH and another patient with near-haploid hypodiploid ALL whose tumor carried a somatic *KDM1A* truncating mutation c.1249C>T (p.Gln417*, MAF 83%). Mouse *Kdm1a*$^{-/-}$ LSK hematopoietic stem-progenitor cells have upregulated HOXA9 and LSK leukemia stem cell signatures (25). Reanalysis of *KDM1A*-mutant and wt hypodiploid ALL tumor transcriptomes revealed that *KDM1A* mutations enriched for these same leukemia stem cell signatures (Supplementary Fig. S2; ref. 25). In addition, query of germline sequence data from The Cancer Genome Atlas revealed germline truncating and splice-site *KDM1A* mutations in 3 patients with glioblastoma multiforme (*KDM1A* c.2371C>T [p.Gln791*]), glioma, and ovarian serous cystadenocarcinoma (both *KDM1A* c.1476+1_1476+2delGT [p.Met448_Lys492del]). Thus, our data are consistent with *KDM1A* mutations contributing to predisposition of other tumors in addition to multiple myeloma.

Disclosure of Potential Conflicts of Interest

K.E. Nichols reports receiving commercial research grants from Incyte and Alpine Biosciences. L.A. Godley has provided expert testimony for UpToDate, Inc. J.E. Garber reports receiving commercial research support from Novartis Pharmaceuticals, is a consultant/advisory board member for Novartis Pharmaceuticals, GTC Pharmaceuticals, and Helix Genetics, and has provided expert testimony for Oric Pharmacetuicals. C.G. Mullighan reports receiving commercial research grants from Loxo Oncology, Pfizer, and Abbvie, has received speakers bureau honoraria from Amgen, and is a consultant/advisory board member for Genome Quebec and Cancer Science Institute. No potential conflicts of interest were disclosed by the other authors.

Authors' Contributions

Conception and design: X. Wei, M.N. Calvo-Vidal, V. Joseph, C.M. Vachon, S. Chen-Kiang, M. Salama, N.J. Camp, R.J. Klein, L. Cerchietti, S.M. Lipkin
Development of methodology: X. Wei, M.N. Calvo-Vidal, J. Zhang, M.F. Walsh, K. Curtin, R.J. Klein, H. Yu, L. Cerchietti
Acquisition of data (provided animals, acquired and managed patients, provided facilities, etc.): X. Wei, M.N. Calvo-Vidal, M.F. Walsh, K.E. Nichols, V. Joseph, C. Snyder, C.M. Vachon, J.D. McKay, D.S. Jayabalan, D. Becirovic, A. Viale, J.M. Phillip, D. Atanackovic, R. Niesvizky, O. Landgren, S.L. Slager, L.A. Godley, J. Churpek, J.E. Garber, C.Dumontet, H.T. Lynch, C.G. Mullighan, N.J. Camp, S.M. Lipkin
Analysis and interpretation of data (e.g., statistical analysis, biostatistics, computational analysis): X. Wei, M.N. Calvo-Vidal, S. Chen, G. Wu, M.V. Revuelta, J. Sun, J. Zhang, M.F. Walsh, V. Joseph, J.D. McKay, M. Artomov, J.M. Phillip, K. Curtin, R. Niesvizky, O. Landgren, K.C. Anderson, M.J. Daly, C.G. Mullighan, N.J. Camp, R.J. Klein, H. Yu, S.M. Lipkin
Writing, review, and/or revision of the manuscript: X. Wei, M.N. Calvo-Vidal, S. Chen, M.V. Revuelta, K.E. Nichols, V. Joseph, C. Snyder, C.M. Vachon, D.S. Jayabalan, R.G. Waller, A. Viale, K. Curtin, M. Salama, R. Niesvizky, O. Landgren, S.L. Slager, L.A. Godley, J.E. Garber, K.C. Anderson, C. Dumontet, H.T. Lynch, C.G. Mullighan, N.J. Camp, K. Offit, R.J. Klein, L. Cerchietti, S.M. Lipkin
Administrative, technical, or material support (i.e., reporting or organizing data, constructing databases): X. Wei, S.-P. Wang, D.S. Jayabalan, L.M. Jacobs, R.G. Waller, D. Atanackovic, O. Landgren, R.G. Roeder, N.J. Camp
Study supervision: X. Wei, N.J. Camp, H. Yu, L. Cerchietti, S.M. Lipkin

Acknowledgments

We acknowledge funding from R01 CA167824, R01 CA13464, R01 CA178765, T15 LM007124, R21 CA152336, LLS 6067-09, NCI P30 CA42014, HHSN261201000026C, the V Foundation (V2015-003), the Weill-Cornell Program in Mendelian Genetics, the Utah Genome Project, Huntsman Cancer Institute, Utah Population Database (UPDB), the Utah Cancer Registry (UCR), Icahn School of Medicine at Mount Sinai Office of Research Infrastructure of the NIH award number S10OD018522, and a generous donation from Matthew Bell.

The costs of publication of this article were defrayed in part by the payment of page charges. This article must therefore be hereby marked *advertisement* in accordance with 18 U.S.C. Section 1734 solely to indicate this fact.

Received July 5, 2017; revised November 7, 2017; accepted March 16, 2018; published first March 20, 2018.

References

1. Palumbo A, Anderson K. Multiple myeloma. N Engl J Med 2011;364:1046–60.
2. Schinasi L, Brown E, Camp N, Wang S, Hofmann J, Chiu B, et al. Multiple myeloma and family history of lymphohaematopoietic cancers: results from the International Multiple Myeloma Consortium. Br J Haematol 2016;175:87–101.
3. Chubb D, Weinhold N, Broderick P, Chen B, Johnson DC, Forsti A, et al. Common variation at 3q26.2, 6p21.33, 17p11.2 and 22q13.1 influences multiple myeloma risk. Nat Genet 2013;45:1221–5.
4. Mitchell JS, Li N, Weinhold N, Forsti A, Ali M, van Duin M, et al. Genome-wide association study identifies multiple susceptibility loci for multiple myeloma. Nat Commun 2016;7:12050.
5. Rand KA, Song C, Dean E, Serie DJ, Curtin K, Sheng X, et al. A meta-analysis of multiple myeloma risk regions in African and European ancestry populations identifies putatively functional loci. Cancer Epidemiol Biomarkers Prev 2016;25:1609–18.
6. Swaminathan B, Thorleifsson G, Joud M, Ali M, Johnsson E, Ajore R, et al. Variants in ELL2 influencing immunoglobulin levels associate with multiple myeloma. Nat Commun 2015;6:7213.
7. Halvarsson BM, Wihlborg AK, Ali M, Lemonakis K, Johnsson E, Niroula A, et al. Direct evidence for a polygenic etiology in familial multiple myeloma. Blood Adv 2017;1:619–23.
8. Weinhold N, Meissner T, Johnson D, Seckinger A, Moreaux J, Försti A, et al. The 7p15.3 (rs4487645) association for multiple myeloma shows strong allele-specific regulation of the MYC-interacting gene CDCA7L in malignant plasma cells. Haematologica 2015;100:110–3.
9. Shi YJ, Matson C, Lan F, Iwase S, Baba T, Shi Y. Regulation of LSD1 histone demethylase activity by its associated factors. Mol Cell 2005;19:857–64.
10. Shi Y, Lan F, Matson C, Mulligan P, Whetstine JR, Cole PA, et al. Histone demethylation mediated by the nuclear amine oxidase homolog LSD1. Cell 2004;119:941–53.
11. Lee MG, Wynder C, Cooch N, Shiekhattar R. An essential role for CoREST in nucleosomal histone 3 lysine 4 demethylation. Nature 2005;437:432–5.
12. Metzger E, Wissmann M, Yin N, Muller JM, Schneider R, Peters AH, et al. LSD1 demethylates repressive histone marks to promote androgen-receptor-dependent transcription. Nature 2005;437:436–9.
13. Kircher M, Witten DM, Jain P, O'Roak BJ, Cooper GM, Shendure J. A general framework for estimating the relative pathogenicity of human genetic variants. Nat Genet 2014;46:310–5.
14. Jun G, Flickinger M, Hetrick KN, Romm JM, Doheny KF, Abecasis GR, et al. Detecting and estimating contamination of human DNA samples in sequencing and array-based genotype data. Am J Hum Genet 2012;91:839–48.

15. Manichaikul A, Mychaleckyj JC, Rich SS, Daly K, Sale M, Chen WM. Robust relationship inference in genome-wide association studies. Bioinformatics 2010;26:2867–73.
16. Anderson CA, Pettersson FH, Clarke GM, Cardon LR, Morris AP, Zondervan KT. Data quality control in genetic case-control association studies. Nat Protoc 2010;5:1564–73.
17. Tian YF, Ahn H, Schneider RS, Yang SN, Roman-Gonzalez L, Melnick AM, et al. Integrin-specific hydrogels as adaptable tumor organoids for malignant B and T cells. Biomaterials 2015;73:110–9.
18. Kiziltepe T, Ashley JD, Stefanick JF, Qi YM, Alves NJ, Handlogten MW, et al. Rationally engineered nanoparticles target multiple myeloma cells, overcome cell-adhesion-mediated drug resistance, and show enhanced efficacy *in vivo*. Blood Cancer J 2012;2:e64.
19. de la Puente P, Muz B, Gilson RC, Azab F, Luderer M, King J, et al. 3D tissue-engineered bone marrow as a novel model to study pathophysiology and drug resistance in multiple myeloma. Biomaterials 2015;73:70–84.
20. Dobin A, Davis CA, Schlesinger F, Drenkow J, Zaleski C, Jha S, et al. STAR: ultrafast universal RNA-seq aligner. Bioinformatics 2013;29:15–21.
21. Love MI, Huber W, Anders S. Moderated estimation of fold change and dispersion for RNA-seq data with DESeq2. Genome Biol 2014;15:550.
22. Chen EY, Tan CM, Kou Y, Duan Q, Wang Z, Meirelles GV, et al. Enrichr: interactive and collaborative HTML5 gene list enrichment analysis tool. BMC Bioinformatics 2013;14:128.
23. Boylan KL, Gosse MA, Staggs SE, Janz S, Grindle S, Kansas GS, et al. A transgenic mouse model of plasma cell malignancy shows phenotypic, cytogenetic, and gene expression heterogeneity similar to human multiple myeloma. Cancer Res 2007;67:4069–78.
24. Holmfeldt L, Wei L, Diaz-Flores E, Walsh M, Zhang J, Ding L, et al. The genomic landscape of hypodiploid acute lymphoblastic leukemia. Nat Genet 2013;45:242–52.
25. Kerenyi MA, Shao Z, Hsu YJ, Guo G, Luc S, O'Brien K, et al. Histone demethylase Lsd1 represses hematopoietic stem and progenitor cell signatures during blood cell maturation. Elife 2013;2:e00633.
26. Rudolph T, Beuch S, Reuter G. Lysine-specific histone demethylase LSD1 and the dynamic control of chromatin. Biol Chem 2013;394:1019–28.
27. Linderman MD, Brandt T, Edelmann L, Jabado O, Kasai Y, Kornreich R, et al. Analytical validation of whole exome and whole genome sequencing for clinical applications. BMC Med Genomics 2014;7:20.
28. Petrovski S, Todd JL, Durheim MT, Wang Q, Chien JW, Kelly FL, et al. An exome sequencing study to assess the role of rare genetic variation in pulmonary fibrosis. Am J Respir Crit Care Med 2017;196:82–93.
29. Ji X, Kember RL, Brown CD, Bucan M. Increased burden of deleterious variants in essential genes in autism spectrum disorder. Proc Natl Acad Sci U S A 2016;113:15054–9.
30. Miller A, Asmann Y, Cattaneo L, Braggio E, Keats J, Auclair D, et al. High somatic mutation and neoantigen burden are correlated with decreased progression-free survival in multiple myeloma. Blood Cancer J 2017;7:e612.
31. Lopez-Corral L, Corchete LA, Sarasquete ME, Mateos MV, Garcia-Sanz R, Ferminan E, et al. Transcriptome analysis reveals molecular profiles associated with evolving steps of monoclonal gammopathies. Haematologica 2014;99:1365–72.
32. Sprussel A, Schulte JH, Weber S, Necke M, Handschke K, Thor T, et al. Lysine-specific demethylase 1 restricts hematopoietic progenitor proliferation and is essential for terminal differentiation. Leukemia 2012;26:2039–51.
33. Subramanian A, Tamayo P, Mootha VK, Mukherjee S, Ebert BL, Gillette MA, et al. Gene set enrichment analysis: a knowledge-based approach for interpreting genome-wide expression profiles. Proc Natl Acad Sci U S A 2005;102:15545–50.
34. Bouchard C, Thieke K, Maier A, Saffrich R, Hanley-Hyde J, Ansorge W, et al. Direct induction of cyclin D2 by Myc contributes to cell cycle progression and sequestration of p27. EMBO J 1999;18:5321–33.
35. Tagde A, Rajabi H, Bouillez A, Alam M, Gali R, Bailey S, et al. MUC1-C drives MYC in multiple myeloma. Blood 2016;127:2587–97.
36. Shah V, Sherborne AL, Walker BA, Johnson DC, Boyle EM, Ellis S, et al. Prediction of outcome in newly diagnosed myeloma: a meta-analysis of the molecular profiles of 1905 trial patients. Leukemia 2018;32:102–10.
37. Schoenhals M, Kassambara A, Veyrune JL, Moreaux J, Goldschmidt H, Hose D, et al. Kruppel-like factor 4 blocks tumor cell proliferation and promotes drug resistance in multiple myeloma. Haematologica 2013;98:1442–9.
38. Fog CK, Asmar F, Come C, Jensen KT, Johansen JV, Kheir TB, et al. Loss of PRDM11 promotes MYC-driven lymphomagenesis. Blood 2015;125:1272–81.
39. Bindea G, Mlecnik B, Hackl H, Charoentong P, Tosolini M, Kirilovsky A, et al. ClueGO: a Cytoscape plug-in to decipher functionally grouped gene ontology and pathway annotation networks. Bioinformatics 2009;25:1091–3.
40. Tai YT, Anderson KC. Targeting B-cell maturation antigen in multiple myeloma. Immunotherapy 2015;7:1187–99.
41. Wang H, Wang L, Chi PD, Wang WD, Chen XQ, Geng QR, et al. High level of interleukin-10 in serum predicts poor prognosis in multiple myeloma. Br J Cancer 2016;114:463–8.
42. Lohr JG, Stojanov P, Carter SL, Cruz-Gordillo P, Lawrence MS, Auclair D, et al. Widespread genetic heterogeneity in multiple myeloma: implications for targeted therapy. Cancer Cell 2014;25:91–101.
43. Menu E, Kooijman R, Van Valckenborgh E, Asosingh K, Bakkus M, Van Camp B, et al. Specific roles for the PI3K and the MEK-ERK pathway in IGF-1-stimulated chemotaxis, VEGF secretion and proliferation of multiple myeloma cells: study in the 5T33MM model. Br J Cancer 2004;90:1076–83.
44. Shay G, Hazlehurst L, Lynch CC. Dissecting the multiple myeloma-bone microenvironment reveals new therapeutic opportunities. J Mol Med 2016;94:21–35.
45. Jiang Y, Saga K, Miyamoto Y, Kaneda Y. Cytoplasmic calcium increase via fusion with inactivated Sendai virus induces apoptosis in human multiple myeloma cells by downregulation of c-Myc oncogene. Oncotarget 2016;7:36034–48.
46. Nair S, Branagan AR, Liu J, Boddupalli CS, Mistry PK, Dhodapkar MV. Clonal immunoglobulin against lysolipids in the origin of myeloma. N Engl J Med 2016;374:555–61.
47. Landgren O, Shim YK, Michalek J, Costello R, Burton D, Ketchum N, et al. Agent orange exposure and monoclonal gammopathy of undetermined significance: an operation ranch hand veteran cohort study. JAMA Oncol 2015;1:1061–8.
48. Scales M, Chubb D, Dobbins SE, Johnson DC, Li N, Sternberg MJ, et al. Search for rare protein altering variants influencing susceptibility to multiple myeloma. Oncotarget 2017;8:36203–10.
49. Bolli N, Barcella M, Salvi E, D'Avila F, Vendramin A, De Philippis C, et al. Next-generation sequencing of a family with a high penetrance of monoclonal gammopathies for the identification of candidate risk alleles. Cancer 2017;123:3701–8.
50. Togasaki E, Takeda J, Yoshida K, Shiozawa Y, Takeuchi M, Oshima M, et al. Frequent somatic mutations in epigenetic regulators in newly diagnosed chronic myeloid leukemia. Blood Cancer J 2017;7:e559.
51. Harris WJ, Huang X, Lynch JT, Spencer GJ, Hitchin JR, Li Y, et al. The histone demethylase KDM1A sustains the oncogenic potential of MLL-AF9 leukemia stem cells. Cancer Cell 2012;21473–87.

Cancer Research
The Journal of Cancer Research (1916–1930) | The American Journal of Cancer (1931–1940)

AACR American Association for Cancer Research

Germline Lysine-Specific Demethylase 1 (*LSD1/KDM1A*) Mutations Confer Susceptibility to Multiple Myeloma

Xiaomu Wei, M. Nieves Calvo-Vidal, Siwei Chen, et al.

Cancer Res 2018;78:2747-2759. Published OnlineFirst March 20, 2018.